JOURNAL OF SPACECRAFT AND ROCKETS
Vol. 31, No. 3, May–June 1994

Optimization of Spacecraft Orbit and Shielding for Radiation Dose

Michele M. Gates* and Mark J. Lewis†
University of Maryland at College Park, College Park, Maryland 20742

An implementation of the optimization of spacecraft orbit and shielding thickness for the control of exposure from the natural orbital radiation environment is described. Many space missions, such as crewed flights and those carrying sensitive electronics, are constrained by a maximum allowable radiation dose to materials inside the vehicle. Generally, in the event of a radiation dose concern, additional shielding is added for radiation protection, thus adding more mass to the spacecraft. However, a modification to the orbit might also be used reduce the radiation dose, which, depending on the flexibility of the mission design, may provide a more advantageous solution. It is shown with established optimization techniques that there are many combinations of orbits and shieldings that will yield a specific dose. For a given design space, weighting the importance of the various spacecraft and mission design parameters, including shielding thickness and orbital parameters, allows for mission specific optimization, providing a flexible design tool.

Nomenclature

$DOSE_{constrained}$	=	input maximum dose allowable, in rads
$DOSE_{optimum}$	=	dose calculated in optimization, in rads
$G(1)$	=	dose constraint, in rads
OBJ	=	objective function
T	=	target value of design variable
W	=	weighting factor
X	=	design variable

Introduction

KNOWLEDGE of the radiation environment of a spacecraft is essential for mission success. Charged particles can penetrate materials, depositing their energy. Crewed mission analysts must anticipate human exposure. Radiation can cause acute and somatic effects in the skin, eye, heart, lungs, liver, pancreas, and other vital organs. In addition, the ionization of electronic parts can cause failure, both temporarily and permanently. Some protection can be provided for sensitive targets inside the vehicle with material shielding. These concerns make defining the radiation environment an extremely important aspect of each of the mission planning processes.

The trapped radiation environment consists of protons, electrons, helium, carbon, oxygen, and other ions trapped in the Earth's magnetic field. These particles originate from the sun, cosmic rays, and the Earth's plasma sheet and ionosphere. The particles enter the trapping region of the magnetosphere and can become trapped, continually deflected by the magnetic field lines and reflected near the poles, forming the trapped radiation, or Van Allen, belts.[1,3] The trapped particle environment data currently used were mapped out on several spacecraft flights including Explorer, Injun, and Gemini missions. This work incorporates the subsequent proton and electron models, but does not include a cosmic ray model.

Due to the Earth's approximate dipole field being offset and tilted with respect to the rotational axis, the magnetic field strength is lower over the South Atlantic. Here, the radiation belts reach their lowest altitudes. The South Atlantic anomaly can contribute almost all of the dose in low Earth orbit. For details of the magnetic field, proton and electron distributions, and the magnetic field offset, see Ref. 2.

The radiation belts are contained by the highly dynamic magnetic field; consequently, as the magnetic field changes, the belts vary in response. The field strength is decreasing with time, about 27 nT per year on average, and drifting westward at a rate of about 0.27 deg per year.[9] Since the field strength is decreasing with time, the particles trapped in the field lines move with the field—closer to the Earth. Magnetic storms also change the particles' direction and energy. Furthermore, a solar flare event will cause the field to contract further, pushing the field to lower latitudes, altering the shape of the system, and exposing more of the polar latitudes to the free-space environment.[1,3] Many more variations exist, but a complete discussion is beyond the scope of this work.[1] In addition, the atmosphere changes with solar cycle, expanding during periods of active solar activity (solar maximum) and contracting during less active periods (solar minimum).

Solar flares can be a major contributor to radiation levels during a solar maximum. Solar protons travel from the sun at velocities that vary from 275 km/s to over 150,000 km/s after an extremely severe solar flare. During and directly after the occurrence of a flare, protons can arrive at the Earth in large quantities, sometimes greater than 1.0×10^{10} particles/cm^2, and at energies sometimes significantly above the GeV level. On the average, the solar cycle is an eleven year cycle, with approximately 5.5 years in solar minimum and 5.5 years in solar maximum, with the midyears of each being either the most quiet or most active periods. Unfortunately, there is presently no method of predicting the occurrence of a flare, or its composition.

There is a momentum distortion associated with charged particles moving through the magnetic field. This effect increases towards the Earth, distorting the paths of the solar protons and preventing their degree of penetration of the field. The magnetic field lines have characteristic cutoff energies at which protons at and below the energy level usually do not penetrate. The cutoff energy increases toward the Earth, allowing only higher energy protons to penetrate deep into the field. Hence, orbits deep within the magnetic field are better protected from flare protons than those in trajectories providing partial magnetospheric shielding.

Received Aug. 22, 1992; revision received Jan. 25, 1993; accepted for publication April 9, 1993.

*Graduate Research Fellow, Department of Aerospace Engineering; currently Radiation Engineer, Jackson & Tull. Member AIAA.

†Assistant Professor, Department of Aerospace Engineering. Member AIAA.

Calculation of the Radiation Dose

Existing models were integrated into a single program to calculate the radiation dose inside aluminum geometries for specified missions.[5] The codes have been modified to include the change in the Earth's magnetic moment with time, allowing for more accurate predictions for future missions. This scheme is similar to that employed by numerous groups. A diagram showing the programs included is given in Fig. 1.

The external radiation environment is determined by first calculating the orbit in geocentric coordinates. The altitude, longitude, and latitude are determined in steps of one minute over large times to provide sufficient sampling of the environment.[4] The orbiter's position in space must be known in small enough intervals so that the particle fluences/fluxes can be integrated over the entire orbit and variations throughout the orbit will be accounted for. Since the ground track changes with time, a flux/fluence averaged over many orbits gives a good sampling from which to calculate the total dose. Therefore, calculations are also performed over many orbits.

The magnetic field models IGRF1965 for solar minimum, and Hurwitz 1970 for solar maximum, are used to convert the geocentric data points to geomagnetic coordinates (B and L).[4] These models correspond to the time when the data were taken. The dipole moment is calculated for the solar maximum and minimum conditions using the field expansion coefficients corresponding to the previously described models. In addition, the input year 1970 is used for solar maximum and 1964 is used for solar minimum. This procedure accounts for the decrease in the magnetic moment with time.

The trapped proton and electron data, stored in geomagnetic coordinates, are then obtained for each point.[7,8] Because the field is drifting westward, a flux averaged over many orbits is used to obtain the dose. This allows for complete consideration of passage through the South Atlantic anomaly and other areas. These particle models and procedures are used because they have been deemed the most accurate and have been verified with Shuttle dosimetry measurements.[9,10]

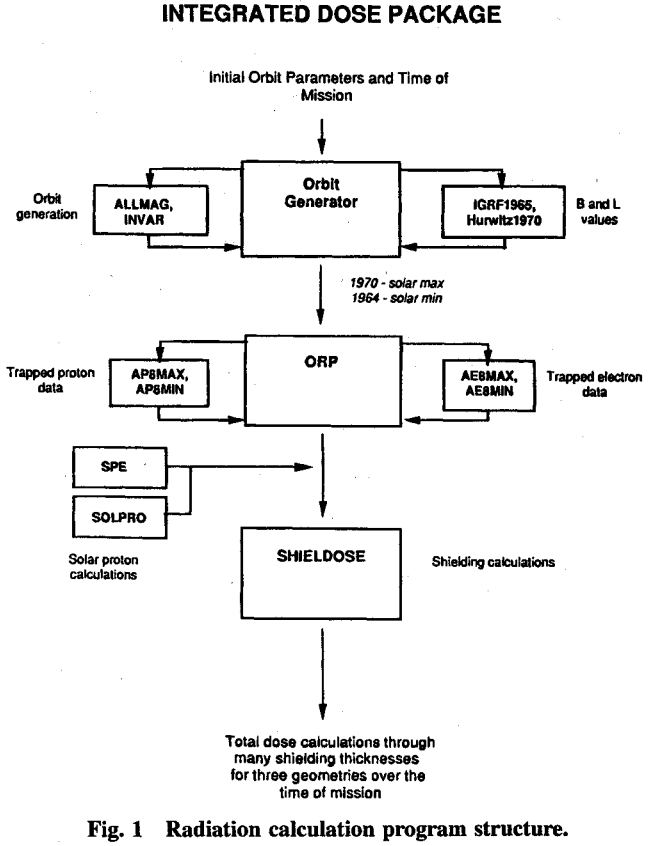

Fig. 1 Radiation calculation program structure.

The free-space solar proton fluence is determined for the entire mission time. The SOLPRO model depends on the length of time spent in solar max and does calculations of fluences for energies up to 100 MeV, which could be extrapolated to higher energy levels.[11] The model is based on satellite measurements from solar cycle 20 and calculates fluences corresponding to the predicted number of flares.

The IGRF1985 model is used to approximate the geomagnetic attenuation of the solar proton environment.[6] The daily percent of time spent in small L-bins is calculated. The cutoff energy corresponding to that of the mean L-value is used to attenuate the free-space spectrum.

At this point, the environment outside of the spacecraft is known. Some of the particles will penetrate the aluminum and irradiate the materials inside. The transport code SHIELDOSE is implemented to calculate the radiation dose on target materials inside aluminum geometries of varying thicknesses.[12] The radiation dose in rads (1 rad = 100 erg/g = .01 Gy) is evaluated in units of silicon, water (human tissue), aluminum, and silicon dioxide. The finite slab, semi-infinite slab, and solid sphere geometries are incorporated. However, the optimization considers the solid sphere geometry only.

Optimization

The optimization procedure is performed by the CONMIN code, which uses a method of feasible directions.[13] The design problem is one of constrained minimization. The target altitude, inclination, and shielding thickness and weighting factors for each are input. Upper and lower bounds for each design variable are also given. The maximum radiation dose is specified as well as the mission variables, such as launch year and day, solar cycle region, and mission length. The design variables include the orbital altitude, angle of inclination, and the aluminum shielding thickness. The objective function is as follows:

$$OBJ = W_1(X_{\text{alt}} - T_{\text{alt}})^2 + W_2(X_{\text{incl}} - T_{\text{incl}})^2 + W_3(X_{\text{sh}} - T_{\text{sh}})^2 \quad (1)$$

where the X values are the design variables, T values are the target values, and the W values are the weighting factors.

The radiation dose constraint is given as follows:

$$G(1) = \left(\frac{\text{DOSE}_{\text{optimum}}}{\text{DOSE}_{\text{constrained}}}\right) - 1 \quad (2)$$

where $DOSE_{\text{optimum}}$ is the calculated radiation dose corresponding to the design variables and the constrained value is given in the input data.

Minimization of the objective function specifies the combination of design variables closest to the target values that yield a radiation dose within the constrained limit. The weighting factors allow for design flexibility. They weigh the importance of how close an optimized design variable is to its target value, allowing analysis of a variety of possible design schemes, depending on the mission objectives. Specified relative to the other design variables, the weighting factors can be set to force the orbit to a target and minimize the shielding for the dose constraint. The factors can also be used to hold the shielding at the desired minimum and vary the orbit to meet the radiation limit.

Results

Figure 2 shows a typical depth-dose curve for a 500-km, 28.5-deg, five-year mission during solar maximum. All of the calculations were performed for solar maximum conditions; however, calculations using the attenuation procedure here found that this orbit is entirely geomagnetically shielded, so solar protons do not contribute to the radiation dose. Electrons are the primary dose contributor at low-shielding thicknesses.

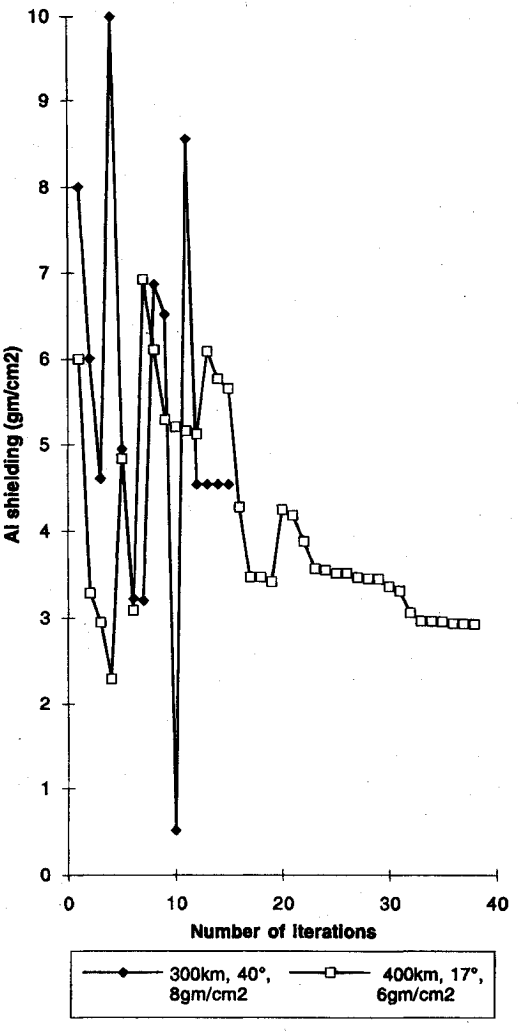

Fig. 8 Iteration histories of shielding thicknesses for unweighted optimizations.

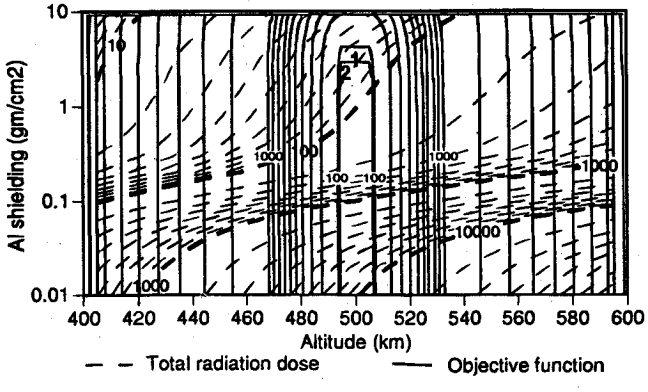

Fig. 9 Unweighted objective function and total dose contours for a five-year mission for varying altitude and shield thickness at 21-deg orbital inclination during solar maximum.

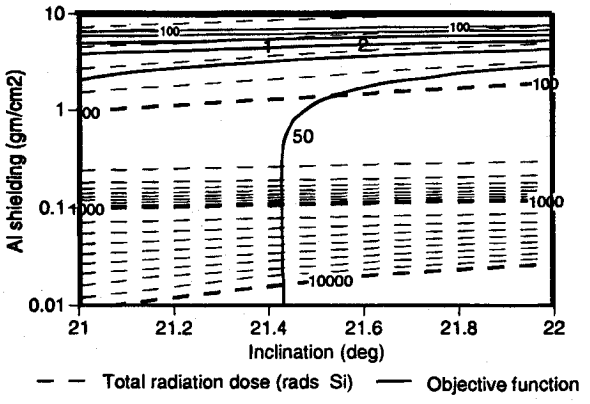

Fig. 10 Unweighted objective function and total dose contours for a five-year mission for 21–22-deg inclination angles at 500 km during solar maximum.

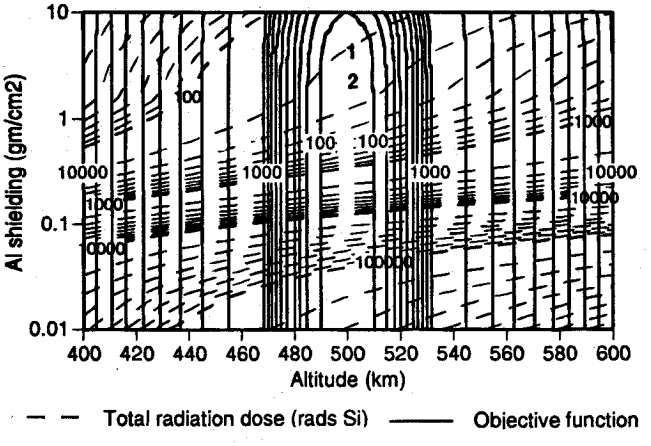

Fig. 11 Weighted objective function and total dose contours for a five-year mission for varying altitude and shield thickness at 28.5-deg orbital inclination during solar maximum.

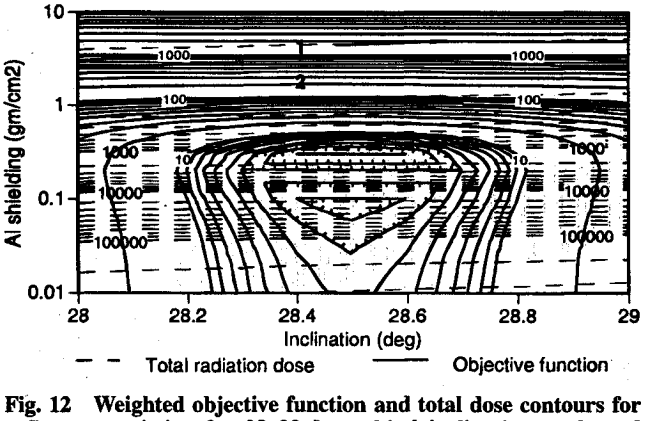

Fig. 12 Weighted objective function and total dose contours for a five-year mission for 28–29-deg orbital inclination angle and varying shield thickness at 500 km during solar maximum.

the target value. The weighting factor for shielding was set to 10 so the gradients would be large enough with respect to shielding for changes in shielding to significantly affect the objective function. The values 1, 10, and 70 were found to produce the desired effect: to hold the orbit as desired and minimize the shielding to meet the radiation requirement. In addition, it was found that since the minimization of shielding increases the radiation dose, the optimized design configuration yields the maximum dose allowable.

Two cases of this weighted optimization were explored. In the first, a maximum dose constraint of 200 rads-Si was implemented. The optimum design was reached in 11 iterations. The final design variables were 499.8 km, 28.4 deg, and 4.567 gm/cm^2 Al, yielding a dose of 200.3 rads-Si. The dose constraint was active at the optimized design. In the second case, 250 rads-S was considered as the maximum allowable dose. The optimization took 13 iterations. The optimum design variables were 499.5 km, 28.4 deg, and 1.986 gm/cm^2 Al, yielding a dose of 250.88 rads-Si. The dose constraint was active at the optimized design.

Figures 11 and 12 present the design space of the 400–500-km orbit at 28–29 deg. Note that in both the altitude/shielding and the inclination/shielding design spaces the weighted objec-

tive function has clearly defined minima. In addition, in the alititude/shielding design space the dose contours are more nonlinear. The final optimized results from the two cases are shown on both figures.

Conclusions

The application of an existing optimization technique, the method of feasible directions, to the space radiation problem provides a flexible tool for the designer. This procedure is applicable in many stages of the design process, from preliminary mission planning to final shielding determination.

With this capability, it is more reasonable to consider incorporation of radiation dose estimates directly into the design of space missions. Forehand knowledge of the radiation dosage can ultimately improve mission design, reduce mission risks, and decrease overall planning time.

It is therefore expected that the availability of a code of this type will have a wide range of applications for spacecraft design including life support, parts analysis, shielding design, trajectory selection, and overall mass requirements.

Acknowledgments

This work was conducted under the support of the NASA Langley Research Center, grant number NAG-1-1285 S-1, with John Nealy as contract monitor. The authors wish to express their gratitude to John Nealy for his significant technical contributions as well. In addition, appreciation is expressed to Bill Atwell of Rockwell International and Christopher Tarpley of the Department of Aerospace Engineering at the University of Maryland for many helpful discussions and suggestions.

References

[1] Jursa, A., *Handbook of Geophysics and the Space Environment,* Air Force Geophysics Lab., Air Force Systems Command, United States Air Force, Hanscom AFB, MA 1985.

[2] Tascione, T., *Introduction to the Space Environment,* Orbit Book Co., Malabar, FL, 1988.

[3] Adams, J. H., Jr., Silberberg, R., and Tsao, C. H., "Cosmic Ray Effects on Microelectronics, Part I: The Near-Earth Particle Environment," Naval Research Lab., NRL Memorandum Rep. 4606, August 1981.

[4] Burrell, M. O., and Wright, J. J., "Orbital Calculations and Trapped Radiation Mapping," NASA TM-53406, March 1966.

[5] Gates, M., Lewis, M. J., and Atwell, W., "A Rapid Method of Calculating the Orbital Radiation Environment," *Journal of Spacecraft and Rockets*, vol. 29, No. 5, 1972, pp. 646–652.

[6] Anon., IAGA Div. I, Working Group 1, "International Geomagnetic Reference Field Revision 1985," *Journal of Geomagnetism and Geoelectricity,* Vol. 37, No. 12, 1985, pp. 1157–1163.

[7] Sawyer, D. M., and Vette, J. I., "AP8 Trapped Electron for Solar Maximum and Solar Minimum," NSSDC 76-06, National Space Science Data Center, Greenbelt, MD, Dec. 1976.

[8] Sawyer, D. M., and Vette, J. I., "The AE8 Trapped Electron Model Environment," NSSDC/WDC-A-R&S 91-24, National Space Science Data Center, Greenbelt, MD, Nov. 1991.

[9] Konradi, A., Hardy, A. C., and Atwell, W., "Radiation Environment Models and the Atmospheric Cutoff," *Journal of Spacecraft and Rockets,* Vol. 24, No. 3, 1987.

[10] Atwell, W., "Astronaut Exposure to Space Radiation: Space Shuttle Experience," SAE Technical Paper Series, No. 901342, July 20, 1990.

[11] Stassinopoulus, E. G., "SOLPRO: A Computer Code to Calculate Probabilistic Energetic Solar Proton Fluences," NSSDC 75-11, National Space Science Data Center, Greenbelt, MD, April 1975.

[12] Seltzer, S., "SHIELDOSE: A Computer Code for Space Shielding Radiation Dose Calculations," U.S. Dept. of Commerce, National Bureau of Standards, NBS TN 1116, May 1980.

[13] Vanderplaats, G. N., and Moses, F., "Structural Optimization by Methods of Feasible Directions," *Journal of Computers and Structures,* Vol. 3, July 1973, pp. 739–755.

Michael E. Tauber
Associate Editor

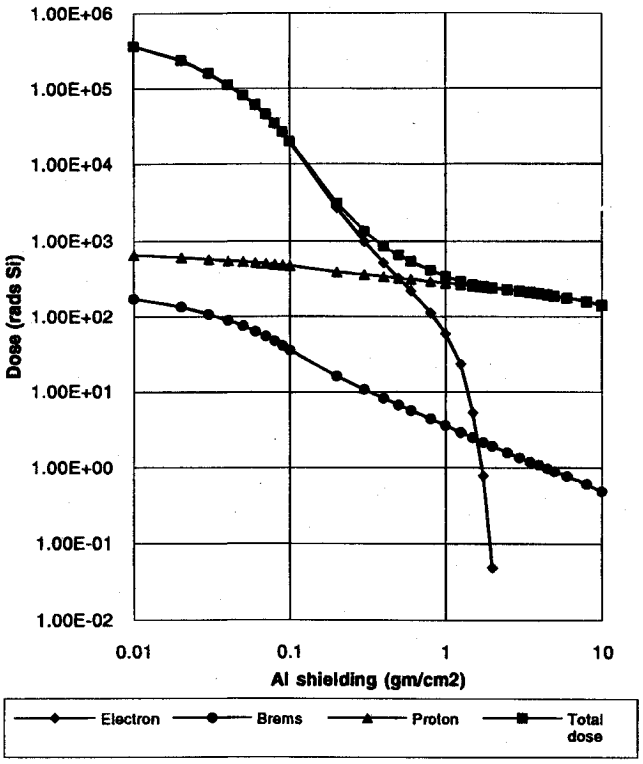

Fig. 2 Total dose results in a silicon target inside a solid aluminum sphere for a five-year mission at 500 km and 28.5 deg in solar maximum.

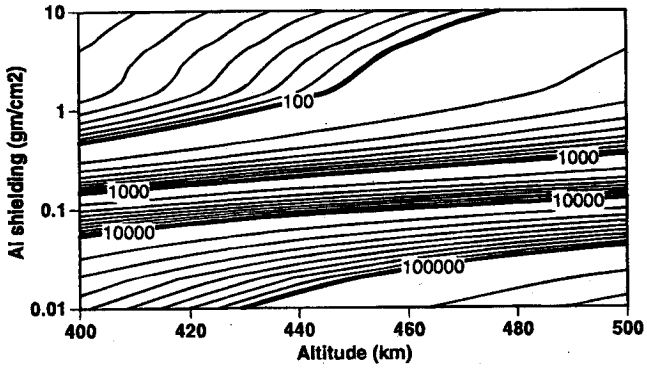

Fig. 3 Total dose contours for 28.5-deg orbits for varying altitudes and shieldings.

Beyond 0.5 gm/cm^2, protons become the dominant mechanism. Electrons are more easily shielded off than protons, causing the slope of the dose curve to decrease significantly in the proton region. This is important in the optimization procedure since shielding is less effective in reducing the dose at higher thicknesses. Secondary effects of the electron transport, labeled bremsstrahlung, propagate though the aluminum far beyond the electrons themselves. This becomes important in orbits where little or no protons are encountered.

Constant dose contours for varying shielding thicknesses, inclinations, and altitudes are presented for familiarization with the design space encountered in this work. Calculations of the radiation dose to a silicon target behind solid aluminum shieldings during five-year missions at solar maximum were performed. The input mission target orbit was 500 km, 28.5 deg with 0.2-gm/cm^2 Al shielding. Total radiation dose contours are shown for 400–500-km altitudes and 0.01–10-gm/cm^2 Al shielding thickness in Fig. 3. The dose contours are only slightly sloped for low shieldings and more variant at higher shieldings. This indicates that the electron environment is approximately

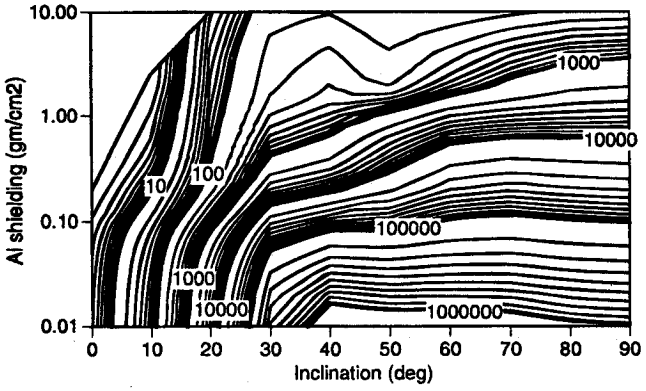

Fig. 4 Total dose contours for 500-km orbits for varying inclinations and shieldings.

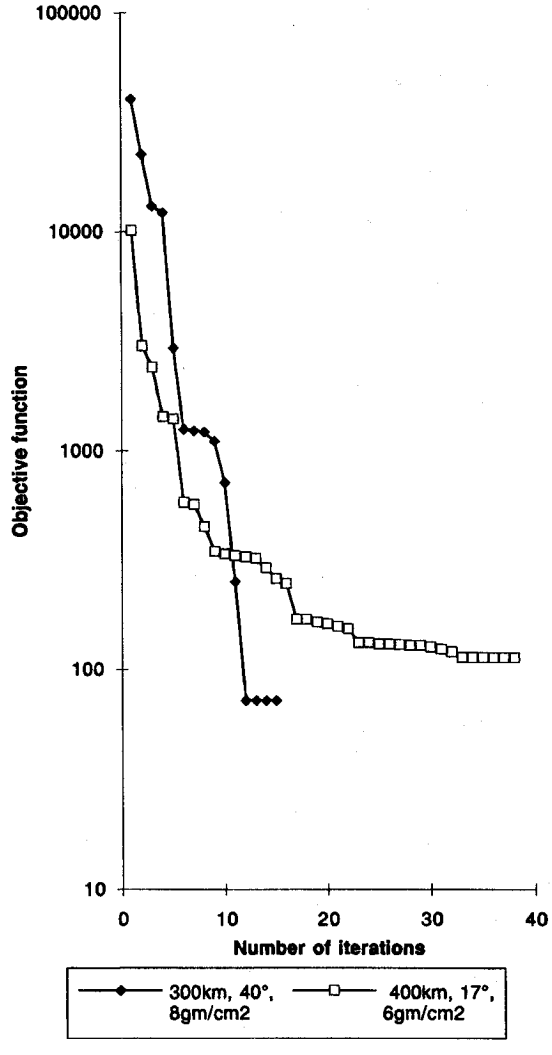

Fig. 5 Iteration histories of objective functions for unweighted optimizations.

constant through this altitude range, but the proton environment is not. In fact, this orbit passes directly through the South Atlantic anomaly where high proton levels are present. Hence, changes in altitude are less significant at low-shielding levels than at higher thicknesses.

Total dose contours are given for 0–90-deg inclination angles at 500 km altitude and the same shielding region as in Fig. 4. Large changes in dose are produced by small inclination variations in low-angle regions, while at high inclination the dose is fairly constant. In addition, at low inclination angles, variations in shielding thickness do not significantly reduce the dose.

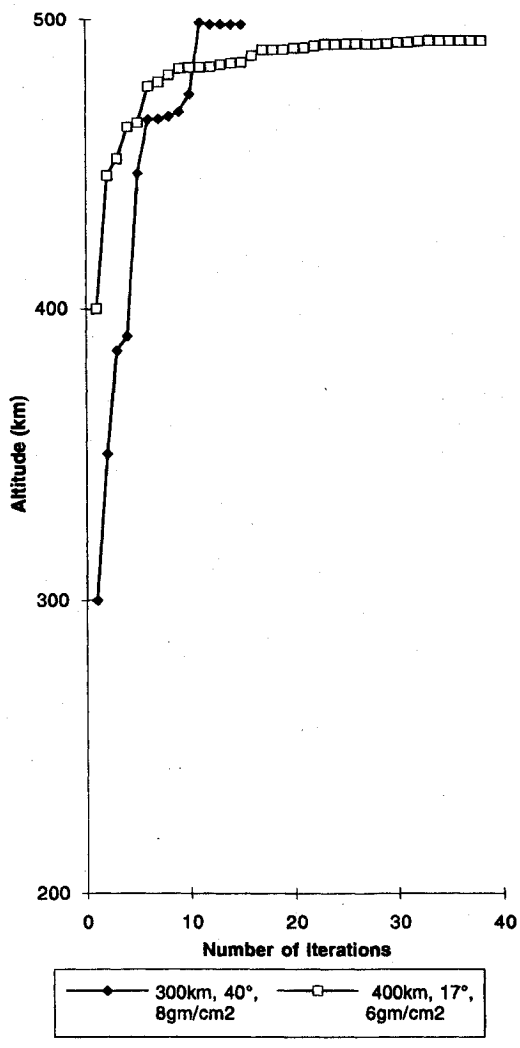

Fig. 6 Iteration histories of altitudes for unweighted optimizations.

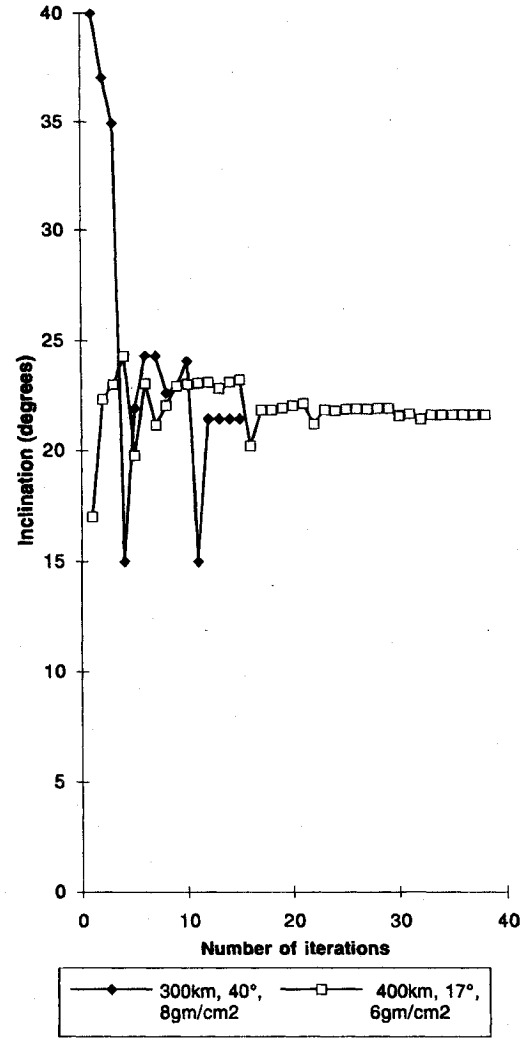

Fig. 7 Iteration histories of inclinations for unweighted optimizations.

The optimization routine was implemented for a target 500-km, 28.5-deg, five-year mission. The target shielding specified was 0.2 gm/cm^2 Al, though unrealistic, to allow the optimizer to minimize the shielding as much as possible. The weighting factors were all set to unity to permit observation of the gradients of the unweighted objective function and resulting search directions. The initial conditions were 300 km at 40 deg and 8 gm/cm^2 Al. The dose limit specified was 75 rads-Si. The optimized solution was reached in 14 iterations. The 498.2-km, 21.4-deg orbit with 4.54 gm/cm^2 Al yielded a total dose of 75.27 rads-Si. The dose constraint was active at the optimum solution. The value $G1$ from Eq. (2) was considered within the dose constraint as long as it was less than 0.01.

Another design case was then optimized for the same target values. The initial conditions were 400 km at 17 deg and 6 gm/cm^2 Al. The optimum solution was reached in 38 iterations. The 492.4 km orbit at 21.6 deg and 2.9 gm/cm^2 Al yielded a total dose of 74.93 rads-Si. The dose constraint was not active at the optimized solution.

The iteration histories of the two optimization cases are shown in Figs. 5–8. The objective function is shown in Fig. 5. Note the quick convergence of the solution where the initial conditions are further from the optimized case. In fact, the objective function for the first case decreased rapidly until the dose constraint became active. Beyond this point, it was not possible to decrease the objective function without violating the constraint. In addition, the objective function for the second case continues to decrease very slightly to the point of the convergence criteria. Figure 6 presents the iteration history of the design variable altitude. The optimized altitudes are approximately equal. The design variable inclination is shown in Fig. 7 and shielding is shown in Fig. 8. The small difference in optimized inclination between the two cases, 0.2 deg, is accounted for in the shielding, about 1.5 gm/cm^2 Al.

The design space for these cases was explored. Figure 9 shows the objective function and dose contours for 400–500-km orbits at 21 deg inclination for varying shielding levels. The minimum occurs at 500 km and 0.2 deg, as expected. Figure 10 shows the objective function and dose contours for 21–22-deg inclination orbits at 500 km for varying shieldings. It is evident that slight changes in inclination, such as 21.4–21.6 deg, have the same effect on dose as changes in shielding levels of 3–4 gm/cm^2, as expected from the results of the optimization. Note that in the altitude/shielding design space, the objective function forms an ellipsoid with a clearly defined minimum and the dose contours are nonlinear. The final optimized results from the two cases are shown on both figures.

A weighted optimization problem was then considered. Here, the orbit is critical to the mission. The same target 500-km, 28.5-deg, five-year mission was input. The target shielding specified was 0.7 gm/cm^2 Al. The initial conditions were 500 km, 28.5 deg, and 8 gm/cm^2 Al. The appropriate weighting factors for this problem were determined after a few iterations. A weighting factor of unity was used for altitude since the altitude stayed constant throughout the unweighted optimization. Since the gradients in objective function with respect to inclination are so large at low inclination, this weighting factor was set to 70. This forced the design inclination to stay near